

Strengthening interacting agegraphic dark energy DGP constraints with local measurements and multimessenger forecastings

Maribel Hernández^{1,*} and Celia Escamilla-Rivera^{1,†}

¹*Instituto de Ciencias Nucleares, Universidad Nacional Autónoma de México,
Circuito Exterior C.U., A.P. 70-543, México D.F. 04510, México.*

An explanation of the nature of dark energy has been treated in extra dimensions within the scheme of string theory. One of the most successful models is inspired by the Dvali-Gabadadze-Porrati (DGP) model, in which the universe is a 4-dimensional brane embedded in a 5-dimensional Minkowski space-time. In this landscape, the study of the evolution of the normal branch has led us to different kinds of dark energy, where the most simple case is the cosmological constant Λ . Moreover, other viable cosmological solutions are related to agegraphic dark energy, which allows a late cosmic acceleration within an interacting mechanism. To explore the viability of these solutions and possible gravitational leakage, in this paper, we present constraints on such models using recent standard sirens forecasting in addition to local observables such as Pantheon (SNIa), $H(z)$ measurements, baryonic acoustic oscillations (BAO). Our results show that the value associated with the species of quantum fields n in these models is strongly restricted for supernovae observations to $n = 20$, and for GW standard sirens mock data prefers a value of $n = 1$.

1. INTRODUCTION

Since the discovery of the late time cosmic acceleration with measurements of Supernovae Type Ia (SNIa) [1, 2], its explanation has been one of the most current intriguing issues in Cosmology. Furthermore, this phenomenon has been attributed to some kind of exotic component so-called *dark energy*, which is characterized by negative pressure and on average constitutes the 70% of content in the Universe.

On this line of thought, the Cosmological Constant Cold Dark Matter (Λ CDM) model assumes that the cosmic acceleration is due to the existence of a Cosmological Constant Λ which Equation-of-State (EoS) is $w_\Lambda = -1$. Although this model has been very successful and well constrained by local [1, 3] and early [4] observables, it has several issues, e.g. the coincidence problem and the small value of Λ [5], and recently, cosmological tensions [6]. In particular, the H_0 tension [7] supports the idea that dark energy could be dynamical with an EoS $w_{DE} < -1$ [8–10]. Among other proposals, dark energy can be associated with terms derived from alternative theories of gravity [11–13] and extended theories of gravity [14, 15], showing a late cosmic acceleration.

Furthermore, different approaches have arisen to explain dark energy within the framework of fundamental theories such as quantum gravity [16] or string theory [17]. Although, until today, there is still not a complete quantum gravity theory, some attempts have been made to discover the nature of dark energy using certain considerations, e.g. through the holographic principle [18] we can propose the *Holographic Dark Energy* (HDE) [19] and employing the Károlyházy relation [20] we derive the *Agegraphic Dark Energy* (ADE) [20]. In the case of the HDE model it has been found cosmological constraints with local observables [21, 22] and with Gravitational Waves (GW) from Einstein Telescope mock data [23]. However, to obtain a cosmic acceleration solution, the length-scale considered in this model is the event horizon [24].

In the case of the ADE model, the time scale is the age of the universe. Originally, this scale was pointed out as an advantage when compared to the HDE model [20]. However, it can be shown that the ADE solution never dominates the dynamics [25]. To solve this drawback, it was proposed two different paths: (i) considering an interaction between the ADE model and dark matter, so-called the ADE interacting model, which modifies the evolution of ADE in such a way that there is a dark energy stage-dominated phase [24]. (ii) The second solution is the *New Agegraphic Dark Energy* (NADE) [25], where the conformal time of the Friedmann-Robertson-Walker (FRW) universe is chosen to be the time scale instead of the age of the universe. Also, it has been considered an interaction scheme with dark matter for this model. The advantage of its description is that is a single-parameter model, unlike the two-parameter ADE model. Furthermore, this NADE model has been constrained with SNIa, Cosmic Microwave Background radiation (CMB), and Large Scale Structure (LSS) data finding better systematics in comparison to the Λ CDM model [26].

*Electronic address: maribel.hernandez@correo.nucleares.unam.mx

†Electronic address: celia.escamilla@nucleares.unam.mx

In this line of thought, and to obtain general solutions that behave as dark energy, it has been proposed the existence of extra-dimensions within the framework of string theory, one of these is the so-called Dvali-Gabadadze-Porrati (DGP) model. In this scheme, the universe is a 4-dimensional brane embedded in a 5-dimensional Minkowski space-time [27] where gravity is modified at cosmological distances. Depending on how the brane is embedded into the space-time bulk, there are two kinds of cosmological solutions. In the well-known self-accelerating branch, we have a matter or radiation epoch that is followed by a late phase of accelerated expansion, while in the normal branch, there is not an accelerated phase and it is necessary to add some kind of dark energy to obtain it [27]. Nevertheless, the self-accelerating branch is disfavoured by SNIa and BAO [28] and this has led to focus the attention on the study of the evolution of the normal branch considering several cases, e.g. a Λ [29], the HDE model [30], the ADE and NADE models [31], and quintessence model [32]. Specifically in [33] the evolution of the ADE model was studied within the framework of DGP brane-world cosmology considering an interaction between this ADE and dark matter. Using a dynamical system analysis, it is possible to find two critical points: an unstable point that is related to a matter-dominated era, and a second point related to an ADE-dominated era that is stable if the coupling parameter that determines the strength of interaction satisfies $\beta < 1 - 2/(3n)$. This means that interaction could lead to a stable universe in the future, contrary to what happens in a DGP brane with non-interacting ADE, which does not have any stable critical point [31]. Also, it was shown that there is no big-rip singularity in this model, in opposition to what happens in a DGP brane with HDE, which suffers from the big-rip singularity [34]. In this analysis, the cosmological parameters were constrained using independent measurements such as SNIa and Baryon Acoustic Oscillations (BAO) peaks, and it was found that these observations prefer a pure holographic dark energy or a pure DGP model [34].

Furthermore, ADE and NADE models have been studied within the DGP braneworld scheme without considering interaction with dark matter, and its cosmological parameters have been constrained with $H(z)$ measurements, CMB, and BAO [31]. In both scenarios, it was found that the universe undergoes an acceleration stage without entering the phantom regime, while in the matter-dominated effective dark energy vanishes. However, as far as we know, these models have not been studied with interaction terms that could lead to gravitational leakage effects. Therefore, in this paper, we studied these models by constraining them using current SNIa measurements (Pantheon (SN)) and standard sirens mock data [35, 36] based on the Laser Interferometer Space Antenna (LISA) by forecasting multimessenger measurements of massive black hole binary (MBHB) mergers. Also, we will include in the analysis local measurements baselines as $H(z)$ measurements, and baryonic acoustic oscillations (BAO).

The paper is divided as follows: In Sec.2 we derive the evolution equations for the ADE and NADE models in a DGP braneworld with interactions. Also, we compute the deceleration parameter for each model. In Sec.3 we describe the observables used to constrain the models described. We include SNIa Pantheon measurements, $H(z)$ measurements, baryonic acoustic oscillations (BAO) and, additionally, a GW mock catalog based on standard sirens. However, since we are dealing with extra-dimensional cosmological models, we need to write a new description of the luminosity distance d_L , in A we derive this function for a D-dimensional space-time to obtain the luminosity gravity wave distance and also, we describe the GW data scattered for our DGP scenarios. In Sec.4 we discuss the statistical analysis, and finally in Sec.5 we present our conclusions.

2. AGEGRAPHIC MODELS IN DGP

2.1. Agegraphic dark energy model (ADE).

According to the DGP model, our universe is a brane embedded in a 5-dimensional Minkowski space-time. The consequence of this is related to a crossover scale r_0 that controls the transition between 4-dimensional behaviour to 5-dimensional, i.e. the gravitational potential of a source of mass m is the well-known 4-dimensional gravitational potential $V \approx -Gm/r$ for $r \ll r_0$, and $V \approx -G_{\text{bulk}}m/r^2$ when $r \gg r_0$ [37]. According to [27] the Friedmann equation in the DGP model is

$$H^2 = \left(\sqrt{\frac{\rho}{3M_p^2} + \frac{1}{4r_0^2}} + \epsilon \frac{1}{2r_0} \right)^2, \quad (1)$$

where $H = \dot{a}/a$ is the Hubble parameter, $\epsilon = \pm 1$, and their different values of ϵ correspond to two different embeddings of the brane into the bulk. If $\epsilon = 1$ a phase of matter or radiation cosmology is followed by a late phase of accelerated expansion. This solution is known as the accelerated branch. If $\epsilon = -1$ there is not an accelerated phase and it is necessary to add some kind of dark energy to obtain an accelerated expansion. This solution is known as the normal branch. In this work, we consider the normal branch and assume that the total energy density on the brane is $\rho = \rho_{\text{ADE}} + \rho_{\text{DM}}$, which contains ADE density ρ_{ADE} and dark matter density ρ_{DM} . The Friedmann equation for

this latter case is given by

$$H = \sqrt{\frac{\rho_{\text{ADE}}}{3M_p^2} + \frac{\rho_{\text{DM}}}{3M_p^2} + \frac{1}{4r_0^2}} - \frac{1}{2r_0}. \quad (2)$$

Based on the Károlyházy relation [38], which says that the distance t cannot be known with better accuracy than $\delta t = \gamma t_p^{2/3} t^{1/3}$, where γ is a numerical factor of order unity [39], we can consider that in an over length scale, the space-time consists of cells of $\delta t^3 \approx t_p^2 t$. Therefore, a cell is the minimal detectable unit of space-time over t . Then, using the fact that this cell has a finite time t , due to the time energy uncertainty relation, there exists a minimal cell δt^3 whose energy cannot be smaller than $E_{\delta t^3} \gtrsim t^{-1}$. The energy density of the quantum fluctuations in Minkowski space-time is $\rho_{\text{ADE}} \sim E_{\delta t^3}/\delta t^3 \sim 1/t_p^2 t^2$. If t is the age of the universe, then the ADE density is given by

$$\rho_{\text{ADE}} = \frac{3n^2 M_p^2}{T^2}, \quad \text{where} \quad T = \int_0^a \frac{da}{Ha}, \quad (3)$$

where n^2 is a numerical factor that was introduced to parameterize for example the species of quantum fields or the effect of curved space-time [40]. Differentiating Eq.(3) with respect to cosmic time t we obtain

$$\dot{\rho}_{\text{ADE}} = -2H\rho_{\text{ADE}} \frac{\sqrt{\Omega_{\text{ADE}}}}{n}. \quad (4)$$

For this case, we are going to consider an interaction between dark matter and ADE. Since there is not a fundamental theory that tells us something about Q , previous works introduced specific forms. In our analysis, we study a specific interaction that is preferred by interacting HDE [41], and which has been already studied within the framework of DGP theory in [42]. Then

$$\dot{\rho}_{\text{DM}} + 3H\rho_{\text{DM}} = Q, \quad (5)$$

$$\dot{\rho}_{\text{ADE}} + 3H(1 + w_{\text{ADE}}) \rho_{\text{ADE}} = -Q, \quad (6)$$

where Q is given by

$$Q = 3\beta H \frac{\rho_{\text{ADE}} \rho_{\text{DM}}}{\rho_{\text{ADE}} + \rho_{\text{DM}}}. \quad (7)$$

β is a positive number, as $Q > 0$ energy flows from ADE to a dark matter component. As it is standard, we define the critical density parameters as

$$\Omega_{\text{DM}} = \frac{\rho_{\text{DM}}}{3H^2 M_p^2}, \quad \Omega_{\text{ADE}} = \frac{\rho_{\text{ADE}}}{3H^2 M_p^2} = \frac{n^2}{H^2 T^2}, \quad \Omega_r = \frac{1}{4r_0^2 H^2}, \quad \Omega_k = -\frac{k}{H^2 a^2}, \quad (8)$$

and their corresponding current values, denoted by the subscript 0, are given by

$$\Omega_{0\text{DM}} = \frac{\rho_{0\text{DM}}}{3H_0^2 M_p^2}, \quad \Omega_{0\text{ADE}} = \frac{\rho_{0\text{ADE}}}{3H_0^2 M_p^2} = \frac{n^2}{H_0^2 T_0^2}, \quad \Omega_{0r} = \frac{1}{4r_0^2 H_0^2}, \quad \Omega_{0k} = -\frac{k}{H_0^2 a_0^2}. \quad (9)$$

Using Eq.(8), we can rewrite Eq.(2) as

$$1 = \Omega_{\text{DM}} + \Omega_{\text{ADE}} - 2\sqrt{\Omega_r}, \quad (10)$$

and $\Omega_{\text{DE}} = \Omega_{\text{ADE}} - 2\sqrt{\Omega_r}$ can be interpreted like an effective dark energy term. Defining $-2\sqrt{\Omega_r}$ as $\Omega_{\text{DGP}} = -2\sqrt{\Omega_r}$, we have

$$\Omega_{\text{DE}} = \Omega_{\text{ADE}} - 2\sqrt{\Omega_r} = \frac{\rho_{\text{ADE}}}{3M_p^2 H^2} - \frac{1}{r_0 H} = \Omega_{\text{ADE}} + \Omega_{\text{DGP}}. \quad (11)$$

Combining Eqs.(4)-(5), the ADE EoS parameter is given by

$$w_{\text{ADE}} = -1 + \frac{2}{3n} \sqrt{\Omega_{\text{ADE}}} - \frac{Q}{3H\rho_{\text{ADE}}} = -1 + \frac{2}{3n} \sqrt{\Omega_{\text{ADE}}} - \frac{\beta \Omega_{\text{DM}}}{\Omega_{\text{ADE}} + \Omega_{\text{DM}}}. \quad (12)$$

The evolution of ρ_{ADE} and ρ_{DM} can be found by solving the following set of differential equations:

$$\dot{\rho}_{\text{ADE}} = -2H\rho_{\text{ADE}}\frac{\Omega_{\text{ADE}}}{n}, \quad (13)$$

$$\dot{\rho}_{\text{DM}} = -Q - 3H\rho_{\text{DM}}. \quad (14)$$

In this work, we are going to constrain the model parameter set $\Theta_{\text{ADE}} : \{H_0, n, \Omega_{0r}, \Omega_{0\text{ADE}}, \beta\}$ with observations. Furthermore, when there is no interaction between the components of the dark sector $w_{\text{DM}}^{\text{eff}} = w_{\text{DM}} = 0$, $\rho_{\text{DM}} \propto (1+z)^3$, and $\rho_{\text{DM}}/\rho_{0c} = \Omega_{0\text{DM}}(1+z)^3$, the current critical density is $\rho_{0c} = 3M_p^2 H_0^2$. Otherwise, when there is an interaction $w_{\text{DM}}^{\text{eff}} = -Q/(3H\rho_{\text{DM}})$, and the previous expressions for ρ_{DM} and $\rho_{\text{DM}}/\rho_{0c}$ are no longer satisfied.

In order to fulfill $\rho_{\text{DM}}(z=0) = \rho_{0\text{DM}}$, we assume that

$$\frac{\rho_{\text{DM}}}{3M_p^2 H_0^2} \equiv \Omega_{0\text{DM}} f_A(z), \quad \text{and} \quad \frac{\rho_{\text{ADE}}}{3M_p^2 H_0^2} = \frac{T_0^2}{T^2} \Omega_{0\text{ADE}} = \Omega_{0\text{ADE}} g_A(z), \quad (15)$$

where $f_A(z=0) = 1 = g_A(z=0)$ and $g_A(z) := T_0^2/T^2$. Replacing Eq.(15) in Eqs.(13)-(2) we obtain

$$\frac{df_A}{dz} = 3 \left(\frac{f_A}{1+z} \right) - \frac{\beta \Omega_{0\text{ADE}} g_A f_A}{(1+z)(\Omega_{0\text{ADE}} g_A + \Omega_{0\text{DM}} f_A)}, \quad (16)$$

$$\frac{dg_A}{dz} = \frac{2\sqrt{\Omega_{0\text{ADE}}} g_A^{3/2}}{n(1+z)H} H_0, \quad (17)$$

$$H = H_0 \left(\sqrt{\Omega_{0\text{DM}} f_A(z) + \Omega_{0\text{ADE}} g_A(z) + \Omega_{0r}} - \sqrt{\Omega_{0r}} \right). \quad (18)$$

We can solve numerically the latter equations using the initial condition $f_A(z=0) = g_A(z=0) = 1$, and find the evolution for Ω_{DM} , Ω_{ADE} , Ω_r , from the following equations

$$\Omega_{\text{DM}} = \Omega_{0\text{DM}} f_A(z) \left(\frac{H_0}{H} \right)^2, \quad \Omega_{\text{ADE}} = \Omega_{0\text{ADE}} g_A(z) \left(\frac{H_0}{H} \right)^2, \quad \Omega_r = \Omega_{0r} \left(\frac{H_0}{H} \right)^2, \quad (19)$$

and using Eqs.(19)-(18) we can compute the deceleration parameter $q = -1 - (\dot{H}/H^2)$ as

$$q = -1 + \frac{H}{H + H_0 \sqrt{\Omega_{0r}}} \left(\frac{3}{2} - \frac{3}{2} \Omega_{\text{ADE}} + \frac{\Omega_{\text{ADE}}^{3/2}}{n} + 3 \frac{H_0}{H} \sqrt{\Omega_{0r}} + \frac{Q}{6M_p^2 H^3} \right). \quad (20)$$

2.2. New Agegraphic dark energy model (NADE).

In this model, the length scale is chosen to be the conformal time $\eta = \int_0^a da/Ha^2$ [25], then the energy density for the NADE model is

$$\rho_{\text{NADE}} = \frac{3n^2 M_p^2}{\eta^2}, \quad \text{and} \quad \Omega_{\text{NADE}} = \frac{n^2}{H^2 \eta^2}. \quad (21)$$

Derivating Eq.(21) with respect to t we obtain

$$\dot{\rho}_{\text{NADE}} = -2\rho_{\text{NADE}} H \frac{\sqrt{\Omega_{\text{NADE}}}}{na}, \quad (22)$$

and considering an interaction between the NADE model and dark matter we have

$$\dot{\rho}_{\text{DM}} + 3H\rho_{\text{DM}} = Q, \quad (23)$$

$$\dot{\rho}_{\text{NADE}} + 3H(1 + w_{\text{NADE}}) \rho_{\text{NADE}} = -Q, \quad (24)$$

where Q is given by Eq.(7). Substituting Eq.(22) in Eq.(23) we can find the EoS for the NADE model

$$w_{\text{NADE}} = -1 + \frac{2}{3na} \sqrt{\Omega_{\text{NADE}}} - \frac{Q}{3H\rho_{\text{NADE}}} = -1 + \frac{2}{3na} \sqrt{\Omega_{\text{NADE}}} - \frac{\beta \Omega_{\text{DM}}}{\Omega_{\text{NADE}} + \Omega_{\text{DM}}}. \quad (25)$$

Finally, we have the following differential equations for ρ_{NADE} and ρ_{DM} ,

$$\dot{\rho}_{\text{NADE}} = -2H\rho_{\text{NADE}}\frac{\Omega_{\text{NADE}}}{n}, \quad (26)$$

$$\dot{\rho}_{\text{DM}} = -Q - 3H\rho_{\text{DM}}, \quad (27)$$

$$H = \sqrt{\frac{\rho_{\text{NADE}}}{3M_p^2} + \frac{\rho_{\text{DM}}}{3M_p^2} + \frac{1}{4r_0^2} - \frac{1}{2r_0}}. \quad (28)$$

We rewrite the latter equations in terms of the model parameters as:

$$\frac{\rho_{\text{DM}}}{3M_p^2 H_0^2} := \Omega_{\text{0DM}} f_N(z) \quad \text{and} \quad \frac{\rho_{\text{NADE}}}{3M_p^3 H_0^2} = \Omega_{\text{0NADE}} g_N(z), \quad (29)$$

where $f_N(z=0) = 1$, $g_N(z=0) = 1$. We find

$$\frac{df_N}{dz} = 3\frac{f_N}{1+z} - \frac{\beta \Omega_{\text{0NADE}} g_N f_N}{(1+z)(\Omega_{\text{0NADE}} g_N + \Omega_{\text{0DM}} f_N)}, \quad (30)$$

$$\frac{dg_N}{dz} = \frac{2\sqrt{\Omega_{\text{0NADE}}} g_N^{3/2}}{nH} H_0, \quad (31)$$

$$H = H_0 \left(\sqrt{\Omega_{\text{0DM}} f_N(z) + \Omega_{\text{0NADE}} g_N(z) + \Omega_{\text{0r}}} - \sqrt{\Omega_{\text{0r}}} \right). \quad (32)$$

As in the ADE model, we can solve numerically the latter equations using the initial condition $f_N(z=0) = g_N(z=0) = 1$, and find the evolution of Ω_{DM} , Ω_{NADE} , Ω_r , from the following equations

$$\Omega_{\text{DM}} = \Omega_{\text{0DM}} f_N(z) \left(\frac{H_0}{H} \right)^2, \quad \Omega_{\text{NADE}} = \Omega_{\text{0NADE}} g_N(z) \left(\frac{H_0}{H} \right)^2, \quad \Omega_r = \Omega_{\text{0r}} \left(\frac{H_0}{H} \right)^2, \quad (33)$$

and q is given by

$$q = -1 + \frac{H}{H + H_0\sqrt{\Omega_{\text{0r}}}} \left(\frac{3}{2} - \frac{3}{2}\Omega_{\text{NADE}} + \frac{(1+z)}{n} \Omega_{\text{NADE}}^{3/2} + 3\frac{H_0}{H} \sqrt{\Omega_{\text{0r}}} + \frac{Q}{6M_p^2 H^3} \right). \quad (34)$$

3. LOCAL OBSERVATIONAL CATALOGS AND FORECASTING BASELINES

In this work, we use four different observational catalogs to constrain the cosmological parameters of the models described. Below we describe them briefly.

- **Pantheon supernovae sample (SNIa).** This catalog contains the information of the apparent magnitude in the B band m_{B} of 1048 supernova events for a redshift range $z = (0.01, 2.26)$. The apparent magnitude m_{B} is related to the observed distance modulus through

$$\mu_{\text{obs}} = m_{\text{B}} - M. \quad (35)$$

For our analysis, we calibrate the absolute magnitude to obtain $M = -19.1$. The theoretical distance modulus μ is related to the luminosity distance, d_L , as follows:

$$\mu(z) = 5 \log \left[\frac{d_L(z)}{1\text{Mpc}} \right] + 25, \quad (36)$$

where $d_L = a_0 c(1+z) \int_0^z dz/H$, and $d/dz (d_L/1+z) = c/H$, with $a_0 = 1$. Notice that d_L is obtained considering that light can only travel along our 4-dimensional space-time and a spatially flat and expanding universe. This luminosity distance is also named d_L^{EM} because is inferred from electromagnetic observations. If light could travel in extra dimensions the luminosity distance would be modified by the presence of these according to Eq.A14.

To perform the statistical analysis, the best-fit parameters for a specific model, using the SN Pantheon catalog, can be calculated by maximising the logarithm of the likelihood function given by

$$\ln \mathcal{L}_{\text{SN}}(\mu_{\text{obs}}(z_i)|z_i, \sigma_i, \Theta) = -\frac{1}{2} \left(\chi_{\text{SN}}^2 + \sum_{n=1}^N \ln(2\pi\sigma_i^2) \right), \quad (37)$$

where Θ denotes the vector of free parameters of the model and

$$\chi_{\text{SN}}^2 = \sum_{i=1}^N \frac{(\mu_{\text{obs}}(z_i) - \mu(z_i; \Theta))^2}{\sigma_i^2}, \quad (38)$$

where σ_i^2 is the variance for each measurement, N is the number of SNIa in the total sample. Using the Bayes theorem we can obtain the joint posterior probability distribution, which is related to the likelihood using

$$p_{\text{SN}}(\Theta|\mu_{\text{obs}}, z, \sigma) = \frac{\pi(\Theta)\mathcal{L}_{\text{SN}}(\mu_{\text{obs}}(z_i)|z_i, \sigma_i, \Theta)}{\varepsilon}, \quad (39)$$

where $\pi(\Theta)$ is the prior probability distribution and ε is the evidence given by

$$\varepsilon = \int d\theta \pi(\Theta) \mathcal{L}_{\text{SN}}(\mu_{\text{obs}}(z_i)|z_i, \sigma_i, \Theta). \quad (40)$$

This is a normalisation constant that is not necessary to compute for the best-fit parameter values. As we can notice, to compute the posterior probability we need to know the prior and compute the likelihood given by Eq.(37).

- **$H(z)$ measurements.** These measurements can offer a tool to obtain constraints on the Hubble rate $H(z)$ at different redshifts z . To use this catalog, we consider the thirty-one data points reported in Ref. [43–46]. This technique involves the use of spectroscopic dating methodologies on passively-evolving galaxies to compute the age difference between two galaxies at different z . When we measure the age difference given by $\Delta z/\Delta t$, we can compute $H(z) = -(1+z)^{-1}\Delta z/\Delta t$. To perform the MCMC analysis, we consider χ_{CC}^2 to compute the agreement between the theoretical Hubble parameter values $H(z_i, \Theta)$, with DGP model parameters, i.e. labelled Θ , and the measured Hubble data values $H_{\text{obs}}(z_i)$, with an error of $\sigma_H(z_i)$. The $\chi_{H(z)}^2$ can be computed through

$$\chi_{H(z)}^2 = \sum_{i=1}^{30} \frac{(H(z_i, \Theta) - H_{\text{obs}}(z_i))^2}{\sigma_H^2(z_i)}. \quad (41)$$

- **Baryonic acoustic oscillations (BAO).** This catalog includes data from the Hubble parameter measurements and the corresponding comoving angular diameter at $z_{\text{eff}} = 0.978, 1.230, 1.526, 1.944$ from SDSS-IV BOSS DR12[47]. For the BAO data mentioned, we calculated the comoving angular diameter distance that is related to the luminosity distance d_L using:

$$D_V(z) = \left[\frac{cz}{H(z)} \frac{d_L(z)^2}{(1+z)^2} \right]. \quad (42)$$

Notice that we require to adopt a fiducial value of $r_{s,\text{fid}}(z_d) = 147.78\text{Mpc}$ and the comoving sound horizon at the baryon drag epoch $r_s(z_d) = 147.6$ [48] Mpc. The statistics can be computed through the χ^2 :

$$\chi_{\text{BAO}}^2(\Theta) = \Delta G(z_i, \Theta)^T C_{\text{BAO}}^{-1} \Delta G(z_i, \Theta), \quad (43)$$

where $\Delta G(z_i, \Theta) = D_V(z_i, \Theta) \times \left(\frac{r_{s,\text{fid}}(z_d)}{r_s(z_d)} \right) - D_{V\text{obs}}(z_i) \times \left(\frac{r_{s,\text{fid}}(z_d)}{r_s(z_d)} \right)$ and C_{BAO} is the corresponding covariance matrix for the BAO observations, and Θ is the same free parameter vector described above.

- **Gravitational Waves mock data.** We use a mock catalog of standard sirens used previously in [49], which consists of standard sirens mock data [35, 36] based on the Laser Interferometer Space Antenna (LISA) by forecasting multimessenger measurements of massive black hole binary (MBHB) mergers. This data was simulated assuming the Λ CDM model, and the best fits are given by the Pantheon catalog with $H_0 = 72.8$ [km/s/Mpc] and $\Omega_m = 0.285$. The mock redshift was generated with the normalised intrinsic merger rate $\dot{n}(z)$, for a range $z \in [0, 2.3]$. The siren distance $D_S(z) = d_L^{\text{GW}}$ that is the GW luminosity distance of the source is given by

$$D_S(z) = D_{S\Lambda\text{CDM}}(z) + \mathcal{N}(0, \sigma), \quad (44)$$

where $\mathcal{N}(0, \sigma)$ is the normal Gaussian probability distribution. The subscript 0 denotes the mean value and σ the standard deviation. The forecasting of this catalog includes 1000 GW d_L of simulated events with their respective redshifts and uncertainties. To employ the full database with the the SNIa sample, we compute the best-fit parameters of the model Θ by maximising the logarithm of the likelihood function given by

$$\ln \mathcal{L}_{\text{GW}}(d_{L_m}^{\text{GW}}(z_i)|z_i, \sigma_i, \Theta) = -\frac{1}{2} \left(\chi_{\text{GW}}^2 + \sum_{n=1}^{1000} \ln(2\pi\sigma_i^2) \right) \quad (45)$$

where

$$\chi_{\text{GW}}^2 = \sum_{i=1}^{1000} \frac{(d_L^{\text{GW}}(z_i, \Theta) - d_{L_m}^{\text{GW}}(z_i))^2}{\sigma_{i_m}^2}. \quad (46)$$

d_L^{GW} is the theoretical GW luminosity distance and $d_{L_m}^{\text{GW}}(z_i)$ is the GW luminosity distance obtained from the forecasting at redshift z_i . The posterior is given by

$$p(\Theta|d_{L_m}^{\text{GW}}, z, \sigma) \propto \pi(\Theta) \mathcal{L}_{\text{GW}}(d_{L_m}^{\text{GW}}(z_i)|z_i, \sigma_i, \Theta). \quad (47)$$

Since within the DGP framework our 4-dimensional brane is embedded in a 5-dimensional Minkowski space-time and gravity propagates through this extra dimension, the gravitational wave distance, the distance measured from gravitational events, e.g. binary BH coalescence differs from the inferred electromagnetic luminosity distance d_L^{EM} . These quantities can be related using the relation Eq.(A19). Therefore, the d_L^{GW} can be rewritten in terms of the DGP model parameters as

$$d_L^{\text{GW}} = d_L^{\text{EM}} \left[1 + \left(2H_0 \sqrt{\Omega_{0r}} \frac{d_L^{\text{EM}}}{c(1+z)} \right)^m \right]^{\frac{1}{2m}}. \quad (48)$$

Finally, considering the combination of the four catalogs described gives the logarithm of the total likelihood function

$$\ln \mathcal{L}_{\text{SN+GW+H}(z)+\text{BAO}} = \ln \mathcal{L}_{\text{SN}} + \ln \mathcal{L}_{\text{GW}} + \ln \mathcal{L}_{\text{H}(z)} + \ln \mathcal{L}_{\text{BAO}}. \quad (49)$$

This is the function we are going to employ to constrain the ADE and NADE models with and without interactions.

4. COSMOLOGICAL CONSTRAINT ANALYSIS

For our statistical analysis of ADE and NADE models in a DGP braneworld cosmology we use the SN Pantheon sample, the mock catalog computed for standard sirens, a 4-data points set from BAO measurements and $H(z)$ 31-data points catalog. Also, we performed a χ^2 -statistics using the combination of these catalogs to estimate the best-fit values of the parameters involved and their corresponding posteriors distributions. In the case of SN observations, to obtain the $\ln \mathcal{L}_{\text{SN}}$ we need to compute the theoretical $\mu(z)$. First, we obtain the luminosity distance d_L . In the case of the ADE model, we solve numerically the set of Eqs.(16)-(17), and finally Eq.(18). For the NADE model, we solve numerically Eqs. (30)-(31). The theoretical $\mu(z)$ is obtained for each redshift z of the sample using Eq.(36). Finally, we compute the $\ln \mathcal{L}_{\text{SN}}$ through Eq.(37) for each model. For the $H(z)$ measurements, we use directly Eq.(41) with the catalog described. And for the BAO measurements, we compute $D_V(z)$ through Eq. (42), respectively, to finally calculate Eq.(43). Finally, we compute the theoretical luminosity GW distance d_L^{GW} for each z_i of the mock catalog using Eq.(48) and derive $\ln \mathcal{L}_{\text{GW}}$ using Eq.(45).

4.1. Results

In this section, we discuss the constraints for the ADE and NADE models considering interacting terms and without them. The statistical analysis is performed using the observational samples described along with the mock data processed with GW configurations.

All statistical confidence levels (C.L) discussed below correspond to 1 and 2σ , respectively. We compute the posteriors of the different models performing a Markov-chain Monte Carlo analysis using the `emcee`¹ code and we combine the marginalized distributions for each fractional density of the models using the `ChainConsumer`² package.

- **ADE without interaction.** In this model $\beta = 0$ in Eq.(16) and the parameters to constrain are $\Theta_{\text{ADE}} = \{\Omega_{0\text{ADE}}, \Omega_{0r}, n, H_0\}$ for SN observations and $\Theta_{\text{ADE}} = \{\Omega_{0\text{ADE}}, \Omega_{0r}, n, H_0, m\}$ for GW's observations. To obtain the priors we consider that the current effective dark energy is $\Omega_{0\text{DE}} = \Omega_{0\text{ADE}} - 2\sqrt{\Omega_{0r}}$ which satisfies $\Omega_{0\text{DM}} + \Omega_{0\text{DE}} = 1$. If $0 < \Omega_{0\text{DE}} < 1$, then $0 < \Omega_{0\text{ADE}} - 2\sqrt{\Omega_{0r}} < 1$, and $0 < 2\sqrt{\Omega_{0r}} < \Omega_{0\text{ADE}} < 1 + 2\sqrt{\Omega_{0r}}$, where if $r_0 > H_0^{-1}$, therefore

$$0 < \Omega_{0r} = \frac{1}{4r_0^2 H_0^2} \leq 0.25 \quad \text{and} \quad 0 < \Omega_{0\text{ADE}} < 2. \quad (50)$$

Furthermore, $\Omega_{0\text{ADE}} = n^2/H_0^2 T_0^2$, where $T_0 = (\int_0^1 da/Ha)^{1/2}$ denotes the age of the universe. Following [50], the age of the Universe lies between $11.2 \text{ Gy} < T_0 < 21 \text{ Gy}$, and the best fit age is $T_0 = 13.14 \text{ Gy}$, therefore if $66 < H_0[\text{km/s/Mpc}] < 74$ then $n \sim 1$. But considering this result $0 < \Omega_{0\text{ADE}} < 2$, and $0 < \Omega_{0r} < 0.25$, then the auto-correlation time is less than τ/N . However, if we reduce the range of the priors for $0 < \Omega_{0\text{ADE}} < 1$, and $0 < \Omega_{0r} < 0.001$, we obtain Gaussian posteriors distributions for $\Omega_{0\text{ADE}}$ and H_0 , with the SN, GW and the combined sample SN+GW. The mean values obtained for the posteriors of these parameters are shown at the bottom of Table I. From this analysis, we obtain that the mean current effective dark energy is higher in comparison to the observations. On the other hand according to [31] $n > 2$, then if we consider the range for the prior for n as $0 < n < 20$ and priors shown at top Table I we get Gaussian C.L for $\Omega_{0\text{ADE}}$ and H_0 , see Figure 4.1. We found that according to the SN Pantheon sample, the most likely value of n tends to its upper limit. This cutoff set a lower current effective dark energy value indicating an older cosmic age. Furthermore, when we combine the full baseline, SN+GW+BAO+H(z), we notice a variation less than 5% on the H_0 bestfits and is even lower for the m parameter $\sim 2\%$. This can be seen in Figure 4.1, where the most probable value for $n \sim 20$. For the GW forecast, the most likely value for $n \sim 1.34$. Although the effective dark energy agrees with observations, computing $T_0 = n/(H_0\sqrt{\Omega_{0\text{ADE}}})$ with the mean values reported at top Table I we found that using SN, GW, and SN+GW data an older cosmic age of the order of hundreds of giga years (Gy). Notice that none of these values matches the estimated age of the Universe [50]. And the crossover scale is on the order of hundreds of Gigaparsecs (Gpc). Therefore, the effect of extra dimension appears at very large distances.

- **ADE with interaction.** We set a flat prior for $0 < \beta < 1$ for this model. This selection is due to the existence of a stable solution for $\beta < 1 - 2/3n$, and $n \geq 1$ [33]. Furthermore, if $\beta > 1$, the evolution of density parameters of dark matter and dark energy deviates from the Λ CDM model at 2σ . The priors considered for the other parameters are shown in Table II and were chosen in such a way that the posterior distributions of $\Omega_{0\text{ADE}}$ and H_0 were Gaussian. We found that GW prefers a greater value of the interacting term β than SN observations, and from their corresponding posterior distributions, it can be seen that the most likely value of β is close to zero for SN data, while for GW data is close to 1. However, the combined data indicates that the most likely value of β is close to zero. From Tables I-II it can be seen that the current effective dark energy $\Omega_{0\text{DE}}$ is lower in comparison to when there is no interacting term. As in the previous case, the posterior for Ω_{0r} is flat for SN and GW observations. In Table II, it can be found that the crossover scale r_0 is on the order of hundreds of Gpc. Furthermore, when we combine the full baseline, SN+GW+BAO+H(z) the m parameter deviates around 1% in comparison to the sample SN+GW, also showing no significant change on H_0 .
- **NADE without interaction.** Unlike the ADE model, in the NADE model, the parameter n is not related to the age of the universe, so we consider the flat prior $0 < n < 20$. We found that to obtain a Gaussian posterior distribution for $\Omega_{0\text{ADE}}$ and H_0 we have to consider the flat priors $0 < \Omega_{0\text{NADE}} < 0.9$ and the ones shown in Table III. For this model, it can be seen that for GW mock data the most likely value of n is close to one while

¹ emcee.readthedocs.io

² samreay.github.io/ChainConsumer

Parameters	Priors	SN	GW	SN+GW	SN+GW+H(z)+BAO
$\Omega_{0\text{ADE}}$	(0,1)	0.785 ± 0.027	0.799 ± 0.095	0.751 ± 0.025	0.755 ± 0.026
Ω_{0r}	(0, 0.0025)	$(12.6 \pm 8.5) \times 10^{-4}$	$(12.6 \pm 8.5) \times 10^{-4}$	$(10.3 \pm 8.2) \times 10^{-4}$	$(9.3 \pm 7.7) \times 10^{-4}$
n	(0,20)	13.5 ± 4.7	4.2 ± 3.0	14.6 ± 4.0	13.3 ± 4.7
H_0 [km/s/Mpc]	(66,74)	71.54 ± 0.23	68.9 ± 1.2	71.33 ± 0.20	71.38 ± 0.2
m	(0.1,2)	-	1.35 ± 0.43	1.71 ± 0.22	1.73 ± 0.2
$\Omega_{0\text{DE}}$	-	$0.714^{+0.006}_{+0.003}$	$0.728^{+0.074}_{-0.064}$	$0.687^{+0.010}_{+0.003}$	$0.694^{+0.010}_{+0.004}$
T_0 [Gyr]	-	$208.384^{+66.954}_{-69.703}$	$66.722^{+39.559}_{-46.053}$	$231.087^{+57.720}_{-59.967}$	$209.806^{+68.595}_{-55.257}$
r_0 [Gpc]	-	$590.686^{+448.153}_{-135.690}$	$613.319^{+480.915}_{-147.484}$	$655.240^{+799.980}_{-167.692}$	$689.085^{+976.907}_{-180.838}$
$\Omega_{0\text{ADE}}$	(0, 1)	0.913 ± 0.031	0.828 ± 0.077	0.812 ± 0.020	0.817 ± 0.022
Ω_{0r}	(0,0.001)	$(4.4 \pm 3.4) \times 10^{-4}$	$(5 \pm 3.4) \times 10^{-4}$	$(2.6 \pm 2.3) \times 10^{-4}$	$(3.5 \pm 3.0) \times 10^{-4}$
n	(0,2)	1.903 ± 0.077	1.42 ± 0.28	1.947 ± 0.042	1.97 ± 0.042
H_0 [km/s/Mpc]	(66, 74)	70.82 ± 0.21	68.32 ± 0.84	70.34 ± 0.18	70.33 ± 0.17
m	(0.1,2)	-	1.31 ± 0.46	1.67 ± 0.24	1.69 ± 0.24
$\Omega_{0\text{DE}}$	-	$0.871^{+0.017}_{-0.009}$	$0.783^{+0.015}_{+0.014}$	$0.795^{+0.35}_{-0.067}$	$0.779^{+0.008}_{+0.001}$
T_0 [Gyr]	-	$27.514^{+0.556}_{-0.573}$	$22.348^{+2.932}_{-3.274}$	$30.053^{+0.199}_{-0.202}$	$30.320^{+0.164}_{-0.166}$
r_0 [Gpc]	-	$1009.738^{+1114.606}_{-253.598}$	$981.879^{+775.461}_{-233.543}$	$1322.519^{+2580.862}_{-361.613}$	$1140.030^{+1883.515}_{-305.494}$

TABLE I: Constraints for the ADE model without interaction. The first column denotes the free parameters of the model, the second column describes the priors considered, and the third-fourth-fifth columns include the constraints for each parameter using SN Pantheon, GW mock data, and the total sample SN+GW, respectively. In the last column, we include the bestfits for the total baseline SN+GW+BAO+H(z). In the sub Table below we include a second option of priors for Ω_{0r} and n . Notice that $\Omega_{0\text{DE}}$ is a derivable parameter and m is not a variable for SN data.

its mean value is $n = 7.4$, GW prefers a smaller value for H_0 than SN. Again, the crossover scale is on the order of hundreds of Gpc but this scale is larger than the values found at the top of Table I and Table II. Furthermore, when we combine the full baseline, SN+GW+BAO+H(z) we notice that there is not a significant change in the H_0 and m values.

- **NADE with interaction.** In this case, to obtain Gaussian posteriors for H_0 and $\Omega_{0\text{ADE}}$, we set the flat priors shown in Table III. The posteriors of the parameters are shown in Figure 4.1 at the bottom right side. This model prefers a lower value of β than the one reported for the ADE model. The effective dark energy obtained is lower and the crossover scale is of the order of Gpc. Notice that this behaviour is almost the same when there is no interaction. The best fit for n and H_0 using SN+GW data are the same for the non-interacting NADE model. Moreover, with GW data this model prefers a lower n value in comparison to the constraints obtained from SN and SN+GW, separately. Finally, when we combine the full baseline, SN+GW+BAO+H(z), the deviations in comparison to the sample SN+GW, for the H_0 and m parameters, are quite small $\sim 1\%$.

5. CONCLUSIONS

In this paper, we explore the observational constraints of interacting and non-interacting Agegraphic Dark Energy (ADE) and New Agegraphic Dark Energy (NADE) models in the normal branch within a DGP brane. Also, we

Parameters	Prior	SN	GW	SN + GW	SN+GW+H(z)+BAO
$\Omega_{0\text{ADE}}$	(0,1)	0.763 ± 0.049	0.720 ± 0.093	0.721 ± 0.047	0.751 ± 0.035
Ω_{0r}	(0, 0.005)	$(2.5 \pm 1.7) \times 10^{-3}$	$(2.6 \pm 1.7) \times 10^{-3}$	$(1.7 \pm 1.4) \times 10^{-3}$	$(1.5 \pm 1.3) \times 10^{-3}$
n	(0,20)	13.7 ± 4.6	5.1 ± 3.9	14.8 ± 3.9	13.9 ± 4.4
$H_0[\text{km/s/Mpc}]$	(66,74)	71.49 ± 0.23	68.9 ± 1.2	71.25 ± 0.20	71.34 ± 0.2
β	(0,1)	0.44 ± 0.33	0.52 ± 0.33	0.38 ± 0.30	0.123 ± 0.097
m	(0,2)	-	1.38 ± 0.41	1.74 ± 0.20	1.75 ± 0.19
$\Omega_{0\text{DE}}$	-	$0.663^{+0.019}_{-0.005}$	$0.618^{+0.063}_{-0.051}$	$0.638^{+0.018}_{+0.001}$	$0.673^{+0.014}_{-0.158}$
$T_0[\text{Gyr}]$	-	$214.649^{+62.932}_{-66.785}$	$85.349^{+53.964}_{-63.447}$	$239.345^{+52.850}_{-56.515}$	$219.977^{+62.320}_{-65.569}$
$r_0[\text{Gpc}]$	-	$419.639^{+324.579}_{-96.918}$	$426.958^{+311.594}_{-100.641}$	$510.601^{+708.294}_{-133.543}$	$542.890^{+948.056}_{-387.896}$

TABLE II: Constraints for the ADE model with interaction. The first column denotes the free parameters of the model, the second column describes the priors considered, and the third-fourth-fifth columns include the constraints for each parameter using SN Pantheon, GW mock data, and the total sample SN+GW, respectively. In the last column, we include the bestfits for the total baseline SN+GW+BAO+H(z). In the sub Table below we include a second option of priors for Ω_{0r} and n . Notice that $\Omega_{0\text{DE}}$ is a derivable parameter and m is not a variable for SN data.

Parameters	Prior	SN	GW	SN+GW	SN+GW+H(z)+BAO
$\Omega_{0\text{NADE}}$	(0, 1)	0.784 ± 0.026	0.750 ± 0.061	0.751 ± 0.023	$0.758 \pm .025$
Ω_{0r}	(0, 0.002)	$(10.1 \pm 6.8) \times 10^{-4}$	$(10.1 \pm 6.8) \times 10^{-4}$	$(8.4 \pm 6.6) \times 10^{-4}$	$(7.9 \pm 6.4) \times 10^{-4}$
n	(0, 20)	13.2 ± 4.9	7.4 ± 5.2	14.4 ± 4.1	12.4 ± 5.2
$H_0[\text{km/s/Mpc}]$	(66, 74)	71.56 ± 0.23	69.84 ± 0.82	71.34 ± 0.20	71.3 ± 0.21
m	(0, 2)	-	1.36 ± 0.41	1.7 ± 0.22	1.72 ± 0.21
$\Omega_{0\text{DE}}$	-	$0.720^{+0.007}_{+0.001}$	$0.686^{+0.042}_{-0.033}$	$0.693^{+0.008}_{+0.003}$	$0.701^{+0.006}_{+0.005}$
$r_0[\text{Gpc}]$	-	$659.569^{+498.040}_{-151.311}$	$675.812^{+520.540}_{-159.426}$	$725.468^{+846.128}_{-184.095}$	$748.493^{+974.315}_{-193.795}$

TABLE III: Constraints for the NADE model without interaction. The first column denotes the free parameters of the model, the second column describes the priors considered, and the third-fourth-fifth columns include the constraints for each parameter using SN Pantheon, GW mock data, and the total sample SN+GW, respectively. In the last column, we include the bestfits for the total baseline SN+GW+BAO+H(z). Notice that $\Omega_{0\text{DE}}$ is a derivable parameter and m is not a variable for SN data.

include an analysis with the NADE to study the dynamics in the conformal time scheme instead of the age of the universe, as in ADE versions. A stable solution within these models is the one related to the evolution of the normal branch, which led us to different possibilities for dark energy. It is possible to recover the standard ΛCDM model in the case of a constant EoS, as we can see from each model in Eqs.12-25, respectively. Furthermore, viable cosmological solutions can be obtained from the ADE model version, which allows us to have a late cosmic acceleration within the interacting mechanism with dark matter.

In the ADE model the value of n is related to the age of the universe, then if $T_0 = 13.4$ Gyr, and $66 < H_0 < 74$, $n \approx 1$. However, when we considered in our analysis a prior within $0 < n < 2$, we found that neither the age of the universe nor the effective dark energy agrees with current observations (see Table I). Furthermore, when we extended the prior $n < 20$, we found that the effective dark energy for the non-interacting and interacting ADE model agrees with observations, and the age of the universe is reduced when there are interactions. Conversely, the NADE model

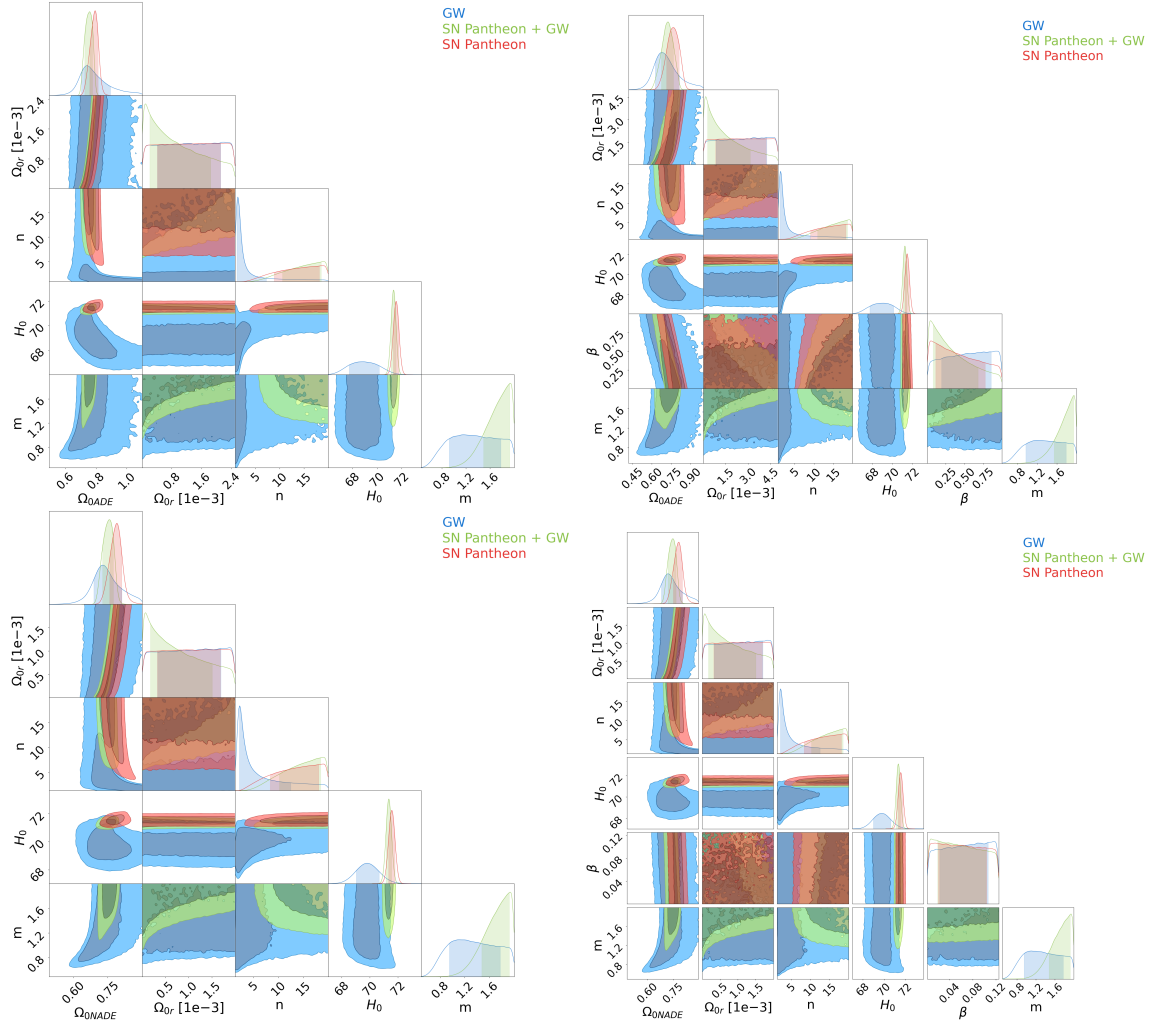


FIG. 1: 2σ C.L. constraints using standard sirens mock data GW (blue), SN Pantheon (red), and the total sample SN Pantheon + GW (green) for the models discussed in Sec.4: *Top left*: ADE without interaction. *Top right*: ADE with interaction. *Bottom left*: NADE without interaction. *Bottom right*: NADE with interaction.

does not have the age drawback because n does not depend on this cosmic age. Furthermore, using the best-fitted values obtained for SN+GW (see Tables I-II-III-IV), we obtain the density parameters evolution of the effective dark energy and dark matter for all models (see Figure 4.1). We found that the evolution of dark matter in these models deviates from the Λ CDM model at $z < 5$. Nevertheless, in the interacting cases, there is more dark matter at present times. Also, we compute their respective deceleration parameters (see Figure 4.1), from where we notice that the universe starts to accelerate at $z = 0.655$ for both non-interacting ADE and NADE models. For the interacting ADE model starts to accelerate at $z \sim 0.37$, and for the interacting NADE model at $z \sim 0.61$. The reason for this behaviour is due to a bigger value of β . According to the constraints obtained using SN+GW data for all models, the best-fit values are $n \sim 14$ and $H_0 \sim 71.3 \text{ km/s/Mpc}$. It is interesting to notice that the evolution of the density parameters in the non-interacting ADE and NADE models are approximately equal and that the evolution of their respective deceleration parameters is practically the same. We also notice that, generally, when we constraint using the total baseline SN+GW+BAO+H(z), there is not a significant change in the constraints reported for the H_0 and m values. The effects of such BAO and H(z) catalogs should be related to the fact that they are calibrated with a concordance standard cosmological model.

For all the models the value for Ω_{0r} is of the order of 10^{-4} . In such a case, r_0 cannot be constrained. Furthermore, the value of n is strongly restricted to an interval between $\{0, 20\}$, where it was found that in the four models, SN observations prefer $n = 20$ and GW mock data prefers a value of $n = 1$. This result implies a younger universe in the ADE model with or without interaction in case we constrain them with GW than SN data.

For all models, GW data prefer a lower value for H_0 than SN data. The value of the current effective dark energy

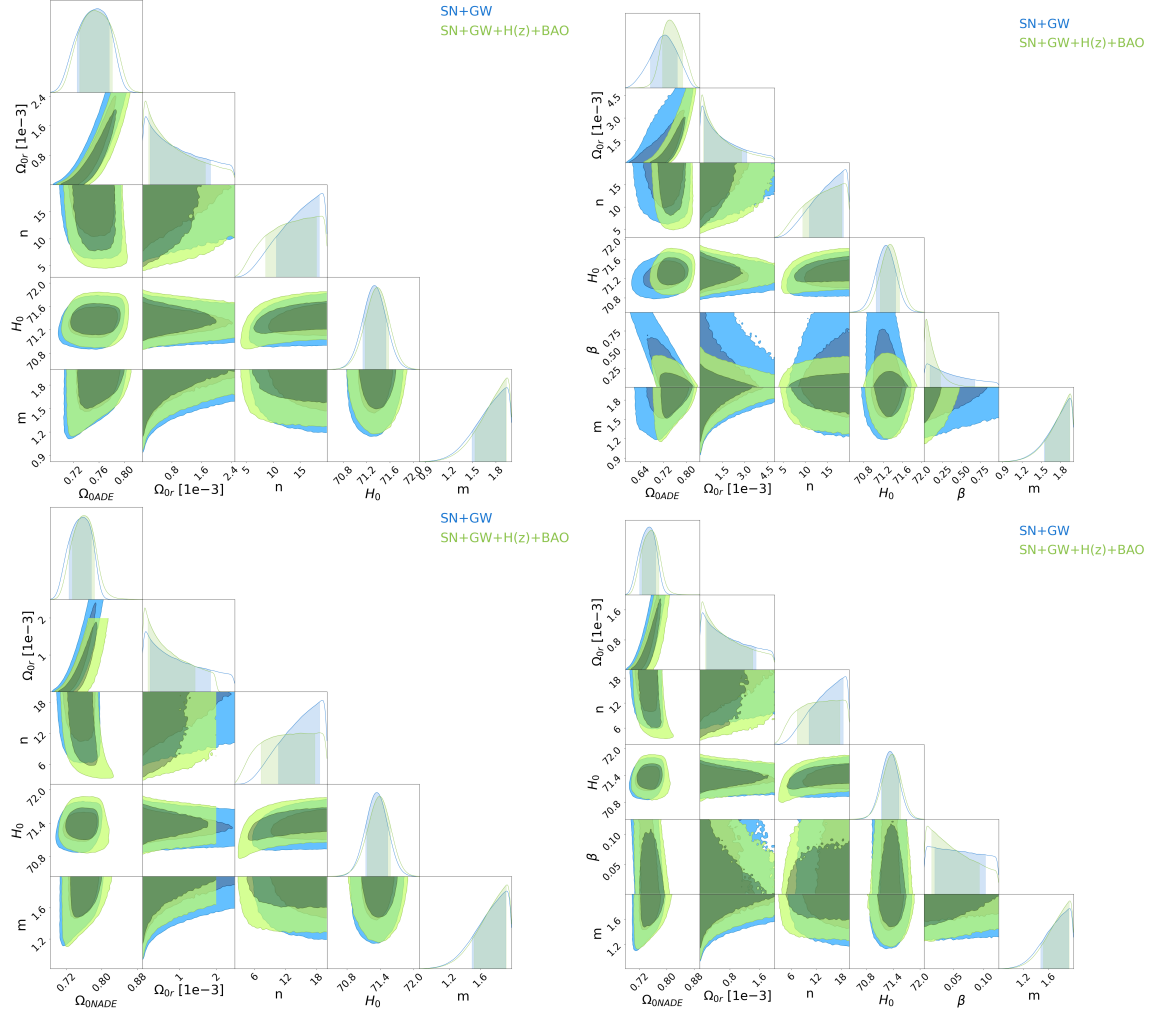


FIG. 2: 2σ C.L constraints using standard sirens mock data GW and SN Pantheon (blue), and the total sample SN+GW+H(z)+BAO (green) for the models discussed in Sec.4: *Top left*: ADE without interaction. *Top right*: ADE with interaction. *Bottom left*: NADE without interaction. *Bottom right*: NADE with interaction.

is less than the value for the case without interaction. In this analysis, we notice that the mean value of the crossover scale is larger, therefore the effects of the extra dimension appear at Gpc scales. At this scale, the dynamics of dark matter do not affect the cosmological evolution in ADE and NADE models.

Acknowledgments

MH acknowledges financial support from SEP-CONAHCYT postgraduate grants program. CE-R acknowledges funding from PAPIIT UNAM Project TA100122 and the Royal Astronomical Society as FRAS 10147. This research has been carried out using computational facilities procured through the Cosmostatistics National Group ICN UNAM project. This article is based upon work from COST Action CA21136 Addressing observational tensions in cosmology with systematics and fundamental physics (CosmoVerse) supported by COST (European Cooperation in Science and Technology).

Appendix A: Luminosity distance for gravitational waves in higher dimensions models

In a Euclidean space, the energy per unit area or flux F , observed by a detector at a certain distance D_L from a source of intrinsic luminosity L is $F = L/4\pi d_L^2$. Taking into account the cosmic expansion in a FRW universe, the

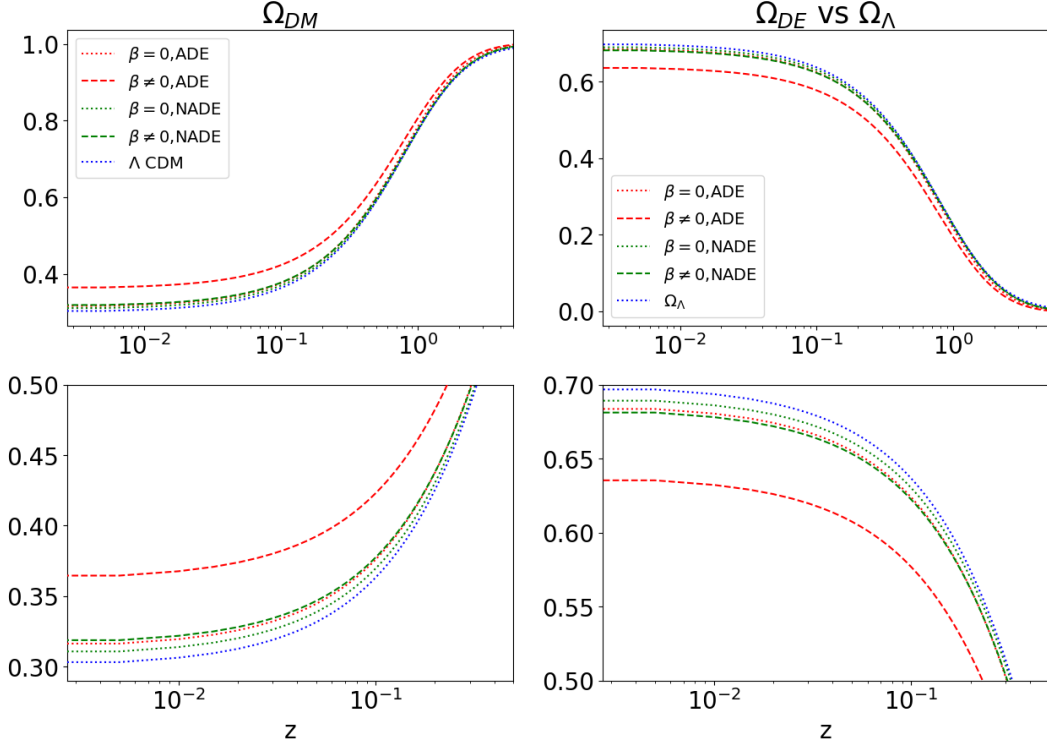


FIG. 3: Comparison of the evolution of density parameters with the Λ CDM model (dotted blue line) using the best-fit values of the parameters obtained from the SN+GW sample. The Λ CDM model is represented by the blue dotted line. For $z > 5$ the evolution of the density parameters is the same as in the Λ CDM model. Each line denotes the models with and without interactions: ADE without interaction (dotted red line), ADE with interaction (dashed red line), NADE without interaction (dotted green line), and NADE with interaction (dashed green line).

Parameters	Prior	SN	GW	SN+GW	SN+GW+H(z)+BAO
$\Omega_{0\text{NADE}}$	(0, 0.9)	0.778 ± 0.027	0.744 ± 0.062	0.743 ± 0.024	0.752 ± 0.025
Ω_{0r}	(0, 0.002)	$(10.1 \pm 6.8) \times 10^{-4}$	$(10.1 \pm 6.8) \times 10^{-4}$	$(8.4 \pm 6.6) \times 10^{-4}$	$(7.8 \pm 6.3) \times 10^{-4}$
n	(0, 20)	13.3 ± 4.8	7.3 ± 5.1	14.4 ± 4.1	12.6 ± 5.1
H_0 [km/s/Mpc]	(66, 74)	71.55 ± 0.23	69.80 ± 0.82	71.33 ± 0.20	71.36 ± 0.21
β	(0, 0.125)	0.067 ± 0.039	0.064 ± 0.042	0.061 ± 0.042	0.053 ± 0.040
m	(0, 2)	-	1.36 ± 0.41	1.70 ± 0.22	1.72 ± 0.21
$\Omega_{0\text{DE}}$	-	$0.714^{+0.008}_{-0.000}$	$0.680^{+0.043}_{-0.035}$	$0.685^{+0.007}_{+0.004}$	$0.696^{+0.006}_{-0.017}$
r_0 [Gpc]	-	$659.661^{+498.110}_{-151.332}$	$676.199^{+520.846}_{-159.521}$	$725.570^{+846.247}_{-184.121}$	$752.643^{+968.712}_{-325.718}$

TABLE IV: Constraints for the NADE model with interaction. The first column denotes the free parameters of the model, the second column describes the priors considered, and the third-fourth-fifth columns include the constraints for each parameter using SN Pantheon, GW mock data, and the total sample SN+GW, respectively. In the last column, we include the bestfits for the total baseline SN+GW+BAO+H(z). Notice that $\Omega_{0\text{DE}}$ is a derivable parameter and m is not a variable for SN data.

luminosity observed is lowered by a factor $1/(1+z)^2$ and the flux is given by

$$F = \frac{L}{4\pi a_0^2 r^2 (1+z)^2}, \quad (\text{A1})$$

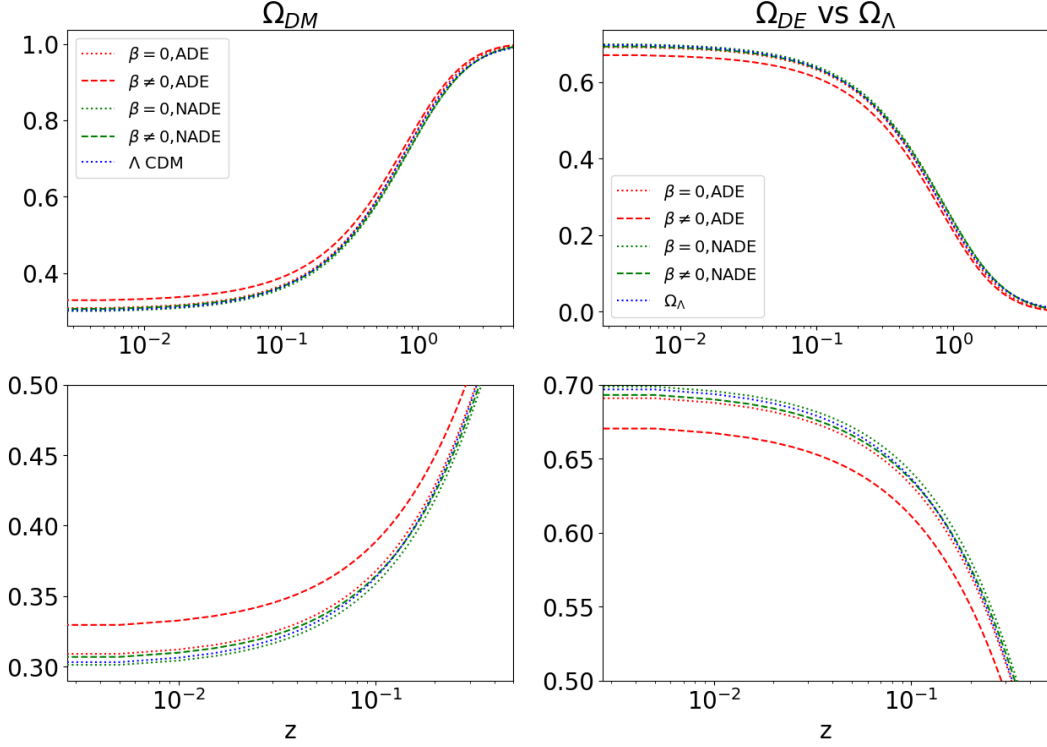


FIG. 4: Comparison of the evolution of density parameters with the Λ CDM model (dotted blue line) using the best-fit values of the parameters obtained from the SN+GW+H(z)+BAO sample. The Λ CDM model is represented by the blue dotted line. For $z > 5$ the evolution of the density parameters is the same as in the Λ CDM model. Each line denotes the models with and without interactions: ADE without interaction (dotted red line), ADE with interaction (dashed red line), NADE without interaction (dotted green line), and NADE with interaction (dashed green line).

where a_0 is the current value of the scale factor and r is the comoving radial distance. From this relationship we establish the luminosity distance in a FRW universe without curvature is

$$d_L = (1 + z)a_0 r. \quad (\text{A2})$$

Considering a $D = N + 1$ -dimensional space with a metric given by

$$ds^2 = -dt^2 + a(t)^2(dr_N^2 + r_N^2 d\Omega_{N-1}^2), \quad (\text{A3})$$

where $d\Omega_{N-1}^2 = d\theta_1^2 + \sin^2 \theta_1 d\theta_2^2 + \sin^2 \theta_1 \sin^2 \theta_2 d\theta_3^2 + \dots + \sin^2 \theta_1 \dots \sin^2 \theta_{N-2} d\theta_{N-1}^2$, the Electromagnetic (EM) flux propagates isotropically in a hypersphere embedded in $N + 1$ dimensions, implying that the relation now defines the luminosity distance in a D -dimensional space

$$F = \frac{L}{S_N}, \quad (\text{A4})$$

where S_N is the area of a N -sphere of radius r_N that can be obtained from integrating the line element at a fixed time and fixed radius r_N as

$$\begin{aligned} S_N &= \int d\theta_1 \dots d\theta_{N-1} \sqrt{-g_{N-1}} \\ &= \int d\theta_1 \dots d\theta_{N-1} r_N^{N-1} a(t)^{N-1} \times \sin^{N-2} \theta_1 \dots \sin^2 \theta_{N-2} \sin \theta_{N-1} \\ &= b_{N-1} r_N^{N-1} a(t)^{N-1}, \end{aligned} \quad (\text{A5})$$

where $b_{N-1} = 2\pi^{N/2}/\Gamma(N/2)$. Therefore

$$F = \frac{L}{b_{N-1} r_N^{N-1} a(t)^{N-1}}. \quad (\text{A6})$$

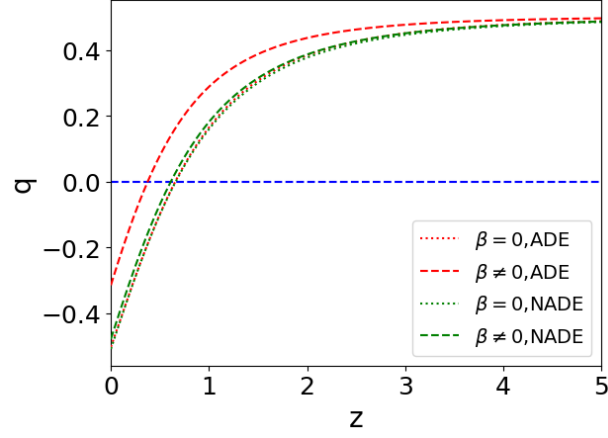


FIG. 5: Deceleration parameter Eqs.(20-34) for ADE and NADE models using the best-fitted values obtained from the combined sample SN+GW. Each line denotes the models with and without interactions: ADE without interaction (dotted red line), ADE with interaction (dashed red line), NADE without interaction (dotted green line), and NADE with interaction (dashed green line). Each line denotes the models with and without interactions: ADE without interaction (dotted red line), ADE with interaction (dashed red line), NADE without interaction (dotted green line), and NADE with interaction (dashed green line).

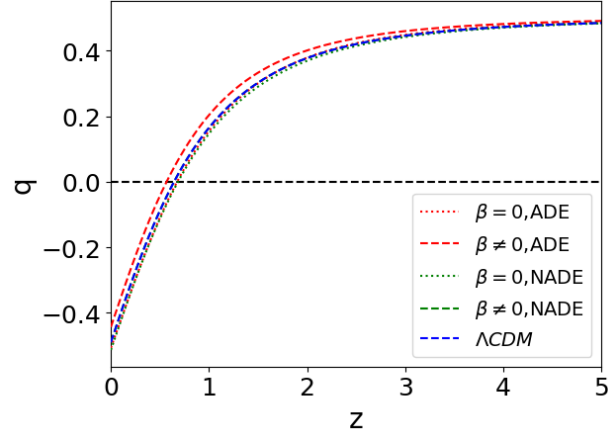


FIG. 6: Deceleration parameter Eqs.(20-34) for ADE and NADE models using the best-fitted values obtained from the combined sample SN+GW+H(z)+BAO. Each line denotes the models with and without interactions: ADE without interaction (dotted red line), ADE with interaction (dashed red line), NADE without interaction (dotted green line), and NADE with interaction (dashed green line) and the Λ CDM model is denoted by the dashed blue line.

Due to the cosmic expansion, the energy of each photon is also redshifted by $1/(1+z)$, this implies that the flux observed at Earth is lowered by a factor $1/(1+z)^2$, then Eq.(A6) is given by

$$F = \frac{L}{b_{N-1} r_N^{N-1} a(t)^{N-1} (1+z)^2} = \frac{L}{b_{N-1} (d_L^D)^{N-1}}, \quad (\text{A7})$$

where d_L^D denotes the luminosity distance for a D -dimensional space-time with metric (A3). From the previous equation

$$d_L^D = a(t) r_N (1+z)^{2/(N-1)} = a(t) r_N (1+z)^{2/(D-2)}. \quad (\text{A8})$$

Furthermore, if we consider in (A3) $ds^2 = 0$ and radial geodesics, then

$$c^2 dt^2 = a(t)^2 dr_N^2, \quad (\text{A9})$$

and from this follows that

$$r_N = c \int_0^z \frac{dz}{H}, \quad (\text{A10})$$

then

$$d_L^{(D)} = a_0 c (1+z)^{\frac{2}{D-2}} \int_0^z \frac{dz}{H}. \quad (\text{A11})$$

The lowest-order waveform of a binary system emitting GWs at cosmological distances in a 4-dimensional universe is

$$h_{\times} = \frac{4}{d_L^4} (G\mathcal{M}_{cz})^{5/3} (\pi f_0)^{2/3} \cos\theta \sin\Phi(t_0), \quad (\text{A12})$$

where h_{\times} is the \times (cross)-polarization of the GW, t_0 and f_0 the time and frequency at the observer, \mathcal{M}_{cz} is the redshifted chirp mass, θ the inclination angle, Φ the GW phase and

$$d_L^4 = a_0 (1+z) r_3, \quad (\text{A13})$$

is the standard 4-dimensional luminosity distance [51]. In the case of extra spatial dimensions, i.e. if we consider the metric given by A3, the waveform of a binary system emitting GWs at cosmological distances in a D-dimensional space-time at the observer is [36]

$$h_{\times} \propto \frac{4}{(1+z)(a_0 r_N)^{(D-2)/2}} (G\mathcal{M}_{cz})^{5/3} (\pi f_0)^{2/3} \cos\theta \sin\Phi(t_0), \quad (\text{A14})$$

and we can rewrite this waveform as

$$h_{\times} \propto \frac{4}{d_L^{\text{GW}}} (G\mathcal{M}_{cz})^{5/3} (\pi f_0)^{2/3} \cos\theta \sin\Phi(t_0). \quad (\text{A15})$$

We defined in the latter equation:

$$d_L^{\text{GW}} \propto (1+z)(a_0 r_N)^{(D-2)/2}, \quad (\text{A16})$$

with $d_L^{\text{GW}} \propto (d_L^D)^{\frac{D-2}{2}}$. In the case of $r_N = r_3$, we can rewrite the above equation as

$$d_L^D = a_0 r_3 (1+z)^{2/(D-2)} = d_L^4 (1+z)^{(4-D)/(D-2)}, \quad (\text{A17})$$

where d_L^4 is the luminosity distance that we can infer from observations denoted by d_L^{EM} , which is the luminosity distance from the electromagnetic signal emitted by a source. Combining the latter equations we obtain

$$d_L^{\text{GW}} \propto d_L^{\text{EM}} \left(\frac{d_L^{\text{EM}}}{1+z} \right)^{\frac{D-4}{2}}. \quad (\text{A18})$$

In the DGP theory, we have a crossover scale r_0 such that if $r \ll r_0$, we recover 4D gravity, and if $r \gg r_0$ the effect of extra-dimensions appears as we can notice for example from the Friedmann equation. Then, to obtain a valid relation at all scales and recover 4-D gravity for $r \ll r_0$ we write

$$d_L^{\text{GW}} = d_L^{\text{EM}} \left[1 + \left(\frac{d_L^{\text{EM}}}{c r_0 (1+z)} \right)^m \right]^{\frac{D-4}{2m}}, \quad (\text{A19})$$

here m determines the steepness of the transition from the small-scale to large-scale behaviour [36]. The value of m is a free parameter and has to be determined by observations, it has to be different from zero.

Notice that the further away the sources and the more pronounced the modification from GR, i.e. the larger the number of dimensions, the lower the screening scale, and the steeper the transition, the larger the discrepancy between the GW and EM luminosity distance and hence the larger the factor by which the error on x^{GW} is increased. To understand this, Fig. 7 shows simulated GW data scattered around their ‘true’ GW distance for both σ stated above for the less ‘extreme’ $\theta^{D=5} : (n=1, H_0)$ and most extreme $\theta^{D=7} : (n=20, H_0)$ cosmological scenarios.

[1] Adam G Riess, Alexei V Filippenko, Peter Challis, Alejandro Clocchiatti, Alan Diercks, Peter M Garnavich, Ron L Gilliland, Craig J Hogan, Saurabh Jha, Robert P Kirshner, et al. Observational evidence from supernovae for an accelerating universe and a cosmological constant. *The astronomical journal*, 116(3):1009, 1998.

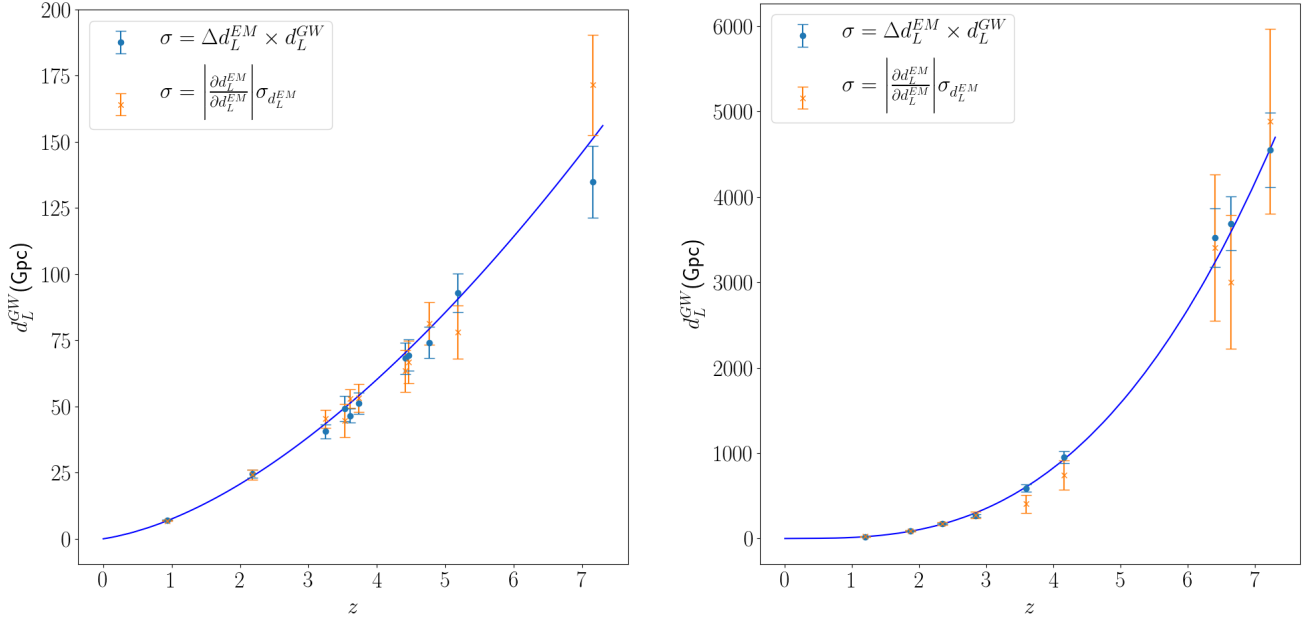


FIG. 7: Examples of GW mock data scattered around their true d_L^{GW} assuming very small (orange) and slightly larger (blue) error bars. *Left*: True cosmological model is characterised by $\theta^{D=5}$: ($m = 1, H_0$). *Right*: True cosmological model is characterised by $\theta^{D=7}$: ($m = 20, H_0$).

- [2] Saul Perlmutter, Goldhaber Aldering, Gerson Goldhaber, RA Knop, Peter Nugent, Patricia G Castro, Susana Deustua, Sebastien Fabbro, Ariel Goobar, Donald E Groom, et al. Measurements of ω and λ from 42 high-redshift supernovae. *The Astrophysical Journal*, 517(2):565, 1999.
- [3] TMC Abbott, M Aguená, A Alarcon, S Allam, O Alves, A Amon, F Andrade-Oliveira, James Annis, S Avila, D Bacon, et al. Dark energy survey year 3 results: Cosmological constraints from galaxy clustering and weak lensing. *Physical Review D*, 105(2):023520, 2022.
- [4] Nabila Aghanim, Yashar Akrami, Mark Ashdown, J Aumont, C Baccigalupi, M Ballardini, AJ Banday, RB Barreiro, N Bartolo, S Basak, et al. Planck 2018 results-vi. cosmological parameters. *Astronomy & Astrophysics*, 641:A6, 2020.
- [5] Steven Weinberg. The Cosmological constant problems. In *4th International Symposium on Sources and Detection of Dark Matter in the Universe (DM 2000)*, pages 18–26, 2 2000.
- [6] Elcio Abdalla et al. Cosmology intertwined: A review of the particle physics, astrophysics, and cosmology associated with the cosmological tensions and anomalies. *JHEAp*, 34:49–211, 2022.
- [7] Eleonora Di Valentino et al. Snowmass2021 - Letter of interest cosmology intertwined II: The hubble constant tension. *Astropart. Phys.*, 131:102605, 2021.
- [8] Celia Escamilla-Rivera and Antonio Nájera. Dynamical dark energy models in the light of gravitational-wave transient catalogues. *JCAP*, 03(03):060, 2022.
- [9] Celia Escamilla-Rivera, Maryi Alejandra Carvajal Quintero, and S. Capozziello. A deep learning approach to cosmological dark energy models. *JCAP*, 03:008, 2020.
- [10] Hai-Chao Zhang. Dynamical dark energy can amplify the expansion rate of the Universe. *Phys. Rev. D*, 107(10):103529, 2023.
- [11] Luisa G. Jaime, Mariana Jaber, and Celia Escamilla-Rivera. New parametrized equation of state for dark energy surveys. *Phys. Rev. D*, 98(8):083530, 2018.
- [12] Timothy Clifton, Pedro G. Ferreira, Antonio Padilla, and Constantinos Skordis. Modified Gravity and Cosmology. *Phys. Rept.*, 513:1–189, 2012.
- [13] Luca Amendola, Radouane Gannouji, David Polarski, and Shinji Tsujikawa. Conditions for the cosmological viability of $f(R)$ dark energy models. *Phys. Rev. D*, 75:083504, 2007.
- [14] Sebastian Bahamonde, Konstantinos F. Dialektopoulos, Celia Escamilla-Rivera, Gabriel Farrugia, Viktor Gakis, Martin Hendry, Manuel Hohmann, Jackson Levi Said, Jurgen Mifsud, and Eleonora Di Valentino. Teleparallel gravity: from theory to cosmology. *Rept. Prog. Phys.*, 86(2):026901, 2023.
- [15] Yi-Fu Cai, Salvatore Capozziello, Mariafelicia De Laurentis, and Emmanuel N. Saridakis. $f(T)$ teleparallel gravity and cosmology. *Rept. Prog. Phys.*, 79(10):106901, 2016.
- [16] Tejinder P. Singh. Dark energy as a large scale quantum gravitational phenomenon. *Mod. Phys. Lett. A*, 35(23):2050195, 2020.
- [17] Paul K. Townsend. Aether, dark energy and string compactifications. *Phil. Trans. Roy. Soc. Lond. A*, 380(2230):20210185, 2021.

2022.

- [18] Shuang Wang, Yi Wang, and Miao Li. Holographic Dark Energy. *Phys. Rept.*, 696:1–57, 2017.
- [19] Shuang Wang, Yi Wang, and Miao Li. Holographic dark energy. *Physics reports*, 696:1–57, 2017.
- [20] Rong-Gen Cai. A dark energy model characterized by the age of the universe. *Physics Letters B*, 657(4-5):228–231, 2007.
- [21] Xing-Wei Qiu, Ze-Wei Zhao, Ling-Feng Wang, Jing-Fei Zhang, and Xin Zhang. A forecast of using fast radio burst observations to constrain holographic dark energy. *JCAP*, 02(02):006, 2022.
- [22] Ryong Gwang Kim and Chang Hyok Ri. Observational constraints on cosmic parameters of holographic dark energy model with varying interaction. *Astrophys. Space Sci.*, 365(7):128, 2020.
- [23] Jing-Fei Zhang, Hong-Yan Dong, Jing-Zhao Qi, and Xin Zhang. Prospect for constraining holographic dark energy with gravitational wave standard sirens from the Einstein Telescope. *Eur. Phys. J. C*, 80(3):217, 2020.
- [24] Hao Wei and Rong-Gen Cai. Interacting agegraphic dark energy. *The European Physical Journal C*, 59:99–105, 2009.
- [25] Hao Wei and Rong-Gen Cai. A new model of agegraphic dark energy. *Physics Letters B*, 660(3):113–117, 2008.
- [26] Hao Wei and Rong-Gen Cai. Cosmological constraints on new agegraphic dark energy. *Physics Letters B*, 663(1-2):1–6, 2008.
- [27] Cedric Deffayet. Cosmology on a brane in minkowski bulk. *Physics Letters B*, 502(1-4):199–208, 2001.
- [28] Malcolm Fairbairn and Ariel Goobar. Supernova limits on brane world cosmology. *Physics Letters B*, 642(5-6):432–435, 2006.
- [29] Varun Sahni and Yuri Shtanov. Braneworld models of dark energy. *Journal of Cosmology and Astroparticle Physics*, 2003(11):014, 2003.
- [30] Xing Wu, Rong-Gen Cai, and Zong-Hong Zhu. Dynamics of holographic vacuum energy in the dgp model. *Physical Review D*, 77(4):043502, 2008.
- [31] H Farajollahi, A Ravanpak, and GF Fadakar. Cosmological constraints on agegraphic dark energy in dgp braneworld gravity. *Astrophysics and Space Science*, 348:253–259, 2013.
- [32] Luis P Chimento, Alejandro S Jakubi, Diego Pavon, and Winfried Zimdahl. Interacting quintessence solution to the coincidence problem. *Physical Review D*, 67(8):083513, 2003.
- [33] Arvin Ravanpak and Golnaz Farpour Fadakar. Interacting agegraphic dark energy model in dgp brane-world cosmology: Dynamical system approach. *Modern Physics Letters A*, 34(14):1950105, 2019.
- [34] Xing Wu, Rong-Gen Cai, and Zong-Hong Zhu. Dynamics of holographic vacuum energy in the dgp model. *Phys. Rev. D*, 77:043502, Feb 2008.
- [35] Maxence Corman, Celia Escamilla-Rivera, and M. A. Hendry. Constraining extra dimensions on cosmological scales with LISA future gravitational wave siren data. *JCAP*, 02:005, 2021.
- [36] Maxence Corman, Abhirup Ghosh, Celia Escamilla-Rivera, Martin A. Hendry, Sylvain Marsat, and Nicola Tamanini. Constraining cosmological extra dimensions with gravitational wave standard sirens: From theory to current and future multimessenger observations. *Phys. Rev. D*, 105(6):064061, 2022.
- [37] Gia Dvali, Gregory Gabadadze, and Massimo Porrati. 4d gravity on a brane in 5d minkowski space. *Physics Letters B*, 485(1-3):208–214, 2000.
- [38] Michael Maziashvili. Space–time in light of károlyházy uncertainty relation. *International Journal of Modern Physics D*, 16(09):1531–1539, 2007.
- [39] Michael Maziashvili. Cosmological implications of karolyhazy uncertainty relation. *Physics Letters B*, 652(4):165–168, 2007.
- [40] Rong-Gen Cai. A dark energy model characterized by the age of the universe. *Physics Letters B*, 657(4):228–231, 2007.
- [41] Lu Feng and Xin Zhang. Revisit of the interacting holographic dark energy model after planck 2015. *Journal of Cosmology and Astroparticle Physics*, 2016(08):072, 2016.
- [42] Arvin Ravanpak and Golnaz Farpour Fadakar. Interacting agegraphic dark energy model in dgp brane-world cosmology: Dynamical system approach. *Modern Physics Letters A*, 34(14):1950105, 2019.
- [43] Michele Moresco, Lucia Pozzetti, Andrea Cimatti, Raul Jimenez, Claudia Maraston, Licia Verde, Daniel Thomas, Annalisa Citro, Rita Tojeiro, and David Wilkinson. A 6% measurement of the Hubble parameter at $z \sim 0.45$: direct evidence of the epoch of cosmic re-acceleration. *JCAP*, 05:014, 2016.
- [44] M. Moresco, A. Cimatti, R. Jimenez, L. Pozzetti, G. Zamorani, M. Bolzonella, J. Dunlop, F. Lamareille, M. Mignoli, H. Pearce, P. Rosati, D. Stern, L. Verde, E. Zucca, C. M. Carollo, T. Contini, J. P. Kneib, O. Le Fèvre, S. J. Lilly, V. Mainieri, A. Renzini, M. Scodeggio, I. Balestra, R. Gobat, R. McLure, S. Bardelli, A. Bongiorno, K. Caputi, O. Cucciati, S. de la Torre, L. de Ravel, P. Franzetti, B. Garilli, A. Iovino, P. Kampczyk, C. Knobel, K. Kovač, J. F. Le Borgne, V. Le Brun, C. Maier, R. Pelló, Y. Peng, E. Perez-Montero, V. Presotto, J. D. Silverman, M. Tanaka, L. A. M. Tasca, L. Tresse, D. Vergani, O. Almaini, L. Barnes, R. Bordoloi, E. Bradshaw, A. Cappi, R. Chuter, M. Cirasuolo, G. Coppa, C. Diener, S. Foucaud, W. Hartley, M. Kamionkowski, A. M. Koekemoer, C. López-Sanjuan, H. J. McCracken, P. Nair, P. Oesch, A. Stanford, and N. Welikala. Improved constraints on the expansion rate of the Universe up to $z \sim 1.1$ from the spectroscopic evolution of cosmic chronometers. *JCAP*, 2012(8):006, 2012.
- [45] Michele Moresco. Raising the bar: new constraints on the Hubble parameter with cosmic chronometers at $z \sim 2$. *Mon. Not. Roy. Astron. Soc.*, 450(1):L16–L20, 2015.
- [46] M. Moresco et al. Improved constraints on the expansion rate of the Universe up to $z \sim 1.1$ from the spectroscopic evolution of cosmic chronometers. *JCAP*, 08:006, 2012.
- [47] Gong-Bo Zhao et al. The clustering of the SDSS-IV extended Baryon Oscillation Spectroscopic Survey DR14 quasar sample: a tomographic measurement of cosmic structure growth and expansion rate based on optimal redshift weights. *Mon. Not. Roy. Astron. Soc.*, 482(3):3497–3513, 2019.

- [48] N. Aghanim et al. Planck 2018 results. VI. Cosmological parameters. *Astron. Astrophys.*, 641:A6, 2020. [Erratum: *Astron. Astrophys.* 652, C4 (2021)].
- [49] Celia Escamilla-Rivera and Antonio Nájera. Dynamical dark energy models in the light of gravitational-wave transient catalogues. *Journal of Cosmology and Astroparticle Physics*, 2022(03):060, 2022.
- [50] Lawrence M Krauss and Brian Chaboyer. Age estimates of globular clusters in the milky way: constraints on cosmology. *Science*, 299(5603):65–69, 2003.
- [51] Michele Maggiore. *Gravitational waves: Volume 1: Theory and experiments*. OUP Oxford, 2007.